A STUDY ON THE PHASE TRANSFORMATION AND EXCHANGE-COUPLING OF $(Nd_{0.95}La_{0.05})_{9.5}Fe_{bal}Co_5Nb_2B_{10.5}$ NANOCOMPOSITES

Q. Chen*, B. M. Ma*, B. Lu**, M. Q. Huang**, D. E. Laughlin**

*Rhodia Inc., Rare Earths and Gallium, CN 7500, Cranbury, New Jersey 08512
**Department of Materials Science and Engineering, Carnegie Mellon University, Pittsburgh, Pennsylvania 15213

ABSTRACT

The phase transformation and the exchange coupling in $(Nd_{0.95}La_{0.05})_{9.5}Fe_{bal}Co_5Nb_2B_{10.5}$ have been investigated. Nanocomposites were obtained by treating amorphous precursors at temperatures ranging from 650°C to 950°C for 10 minutes. The magnetic properties were characterized via the vibrating sample magnetometer (VSM). X-ray diffraction (XRD), thermomagnetic analysis (TMA), and transmission electron microscopy (TEM) were used to perform phase identification, measure grain size, and analyze phase distribution. The strength of the exchange coupling between the magnetically hard and soft phases in the corresponding nanocomposite was analyzed via the ΔM-versus-H plot.

It was found that the remanence (B_r), coercivity (H_{ci}), and maximum energy product (BH_{max}) obtained were affected by the magnetic phases present as well as the grain size of constituent phases and their distribution. The optimal magnetic performance, BH_{max}, occurred between 700°C to 750°C, where the crystallization has completed without excessive grain growth. TMA and TEM indicated that the system was composed of three phases at this point, $Nd_2(Fe\ Co)_{14}B$, α-Fe, and Fe_3B. The exchange coupling interaction among these phases was consistently described via the ΔM-versus-H plot up to 750°C. The B_r, H_{ci}, and BH_{max} degraded severely when the thermal treatment temperature increased from 750°C. This degradation may be attributed to the grain growth of the main phases, from 45 to 68nm, and the development of precipitates, which grew from 5nm at 750°C to 12nm at 850°C. Moreover, the amount of the precipitates was found to increase with the thermal treatment temperatures. The precipitates, presumably borides, may cause a decrease in the amount of the α-Fe and Fe_3B and result in a redistribution of the Co in the nanocomposites. The increase of the Co content in the $Nd_2(Fe\ Co)_{14}B$ may explain the increase of its Curie temperature with the thermal treatment temperatures. In this paper, we examine the impacts of these factors on the magnetic properties of $(Nd_{0.95}La_{0.05})_{9.5}Fe_{bal}Co_5Nb_2B_{10.5}$ nanocomposite.

INTRODUCTION

NdFeB nanocomposite intermetallic compounds have been of great interest of both the scientific community and bonded magnet industry [2-6, 11, 12]. Composed of both magnetically hard and soft phases, nanocomposites usually possess enhanced remanence due to the exchange coupling interaction[2-5]. The overall magnetic performances, namely, remanence (B_r), coercivity (H_{ci}), and maximum energy product ($(BH)_{max}$) are dictated by the strength of the exchange coupling as well as by the magnetic phases present in the nanocomposites.

Using a three dimensional modeling, Schrefl et. al.[5] estimated that the ideal grain size should be approximately 20 nm for the hard phases and 10 nm for the soft phases. Nano-scaled grain size can be achieved by optimal quenching or by over-quenching followed by a crystallization

Mat. Res. Soc. Symp. Proc. Vol. 577 © 1999 Materials Research Society

treatment. It is generally recognized that an increase in the thermal processing temperature results in grain growth. The grain growth usually becomes more rapid at higher temperatures. An excessive grain growth may weaken the exchange coupling and lowers the overall magnetic performance of nanocomposites. However, the impact of the magnetic phase transformation under different thermal processing conditions on the exchange coupling and subsequent magnetic properties have not received the same attention.

The ΔM-versus-H plot has been widely used in the recording media to describe the interacting particle systems [7-9]. This technique can also provide a quantitative means to describe the exchange coupling in the newly developed nanocomposites for permanent magnets [10]. However, due to other factors such as the phase content in the system, the strength of the exchange coupling reflected from the maximum value of ΔM may not be consistently associated with the maximum magnetic performance.

In this work, using a rare-earth-lean and boron-rich NdFeB nanocomposite, $(Nd_{0.95}La_{0.05})_{9.5}Fe_{bal}Co_5Nb_2B_{10.5}$, the phase transformation and the exchange coupling were studied as a function of thermal treatment temperature. Their impact on the magnetic performances, namely, B_r, H_{ci}, $(BH)_{max}$, and $M_{H=18koe}$ (magnetization at 18kOe, an estimation of the saturation magnetization) is reported. The microstructures, including the grain size distribution and development of the intergranular phases, were studied via transmission electron microscopy (TEM). The exchange coupling of the system was investigated via the ΔM-versus-H plot. The main purpose of the study is not to obtain the highest $(BH)_{max}$, but to understand the impact of phase transformation and the strength of the exchange coupling interaction on the magnetic performance from the microstructure point of view.

EXPERIMENTAL

$(Nd_{0.95}La_{0.05})_{9.5}Fe_{bal}Co_5Nb_2B_{10.5}$ ribbons were prepared via the conventional melt-spinning technique. The as-melt-spun materials were isothermally treated in a tube furnace under vacuum (20mtorr) at 650°C, 700°C, 750°C, 850°C, and 950°C. The magnetic properties at room temperature were measured by an EG&G Model 4500 Vibration Sample Magnetometer (VSM) with a maximum applied magnetic field of 18 kOe. All samples were pulse-magnetized at 100 kOe prior to each measurement to mimic hysteresis loop measurement with higher maximum applied field. A Perkin-Elmer Model 7 Thermogravimetric Analyzer (TGA) was modified to perform thermomagnetic analysis (TMA). An X-ray diffractometer (XRD) (Siemens) with Co radiation (λ=1.78897Å) was used to determine the amorphocity of the as-spun materials and phases developed after the thermal treatments.

The exchange interactions of the system were characterized via the ΔM-versus-H plot, in which ΔM (=m_d(H)-(1-2m_r(H), where m_d is the reduced DC magnetization at a given applied magnetic field and m_r is the reduced isothermal remanence) is plotted against the applied magnetic field [7-9].

To carry out microstructure study, as-spun and all thermally treated samples were studied using Phillips-420 transmission electron microscope (TEM) [1]. Samples were prepared by ion milling on a cold stage of a GATAN 600 ion miller. Grain size measurement and phase identification using electron diffraction pattern (EDP) were performed on samples treated with temperatures ranging from 650°C from 850°C.

RESULTS AND DISCUSSIONS

Shown in Figure 1 are the variations of B_r, H_{ci}, BH_{max} and $M_{H=18koe}$, obtained with various thermal processing temperatures. H_{ci} increased from 0.1 kOe in the as-spun state to 1.5 kOe when treated at 650°C, peaked to 11.7 kOe at 700°C then decreased to 8.8 and 7.0 kOe when treated at 750°C and 850°C, respectively. For 950°C, our test resulted in a more dramatic decrease in H_{ci} (to3.3kOe). Unlike H_{ci}, B_r increases from 1.0 kG in the as-spun state to 4.2, 6.8, and 7.0 kG when treated at 650°C, 700°C and 750 °C, respectively. A slight decrease in B_r (from 7.0 to 6.9 kG) was noticed when treated at 850°C. At 950°C, B_r decreased to 5.8 kG. It is of interest to note that H_{ci} reaches the highest value at 700°C, while the highest B_r was obtained when treated between 700°C to 750°C. This difference in optimum values may arise from the fact that two different mechanisms, the exchange coupling, and the phase content, govern H_{ci} and B_r. While exchange coupling is important for both H_{ci} and B_r, the amount of the soft phase competes with the exchange interaction in its effect on B_r. During this competition, B_r can be increased at the expense of reduced exchange interaction and therefore lowered H_{ci}. At 850°C and 950°C, the desired hard and soft magnetic phases may transform into undesired phases and result in the decrease in both H_{ci} and B_r. The trend of BH_{max} is a combined effect of H_{ci} and B_r. BH_{max} begun at 0.0 MGOe in the as-spun state, reached a maximum value of 10.0 MGOe at 700°C and 750°C, and then decreased when treated at a temperature higher than 750°C. Over the course of the study, $M_{H=18kOe}$ exhibited an initial decrease (at 650°C and 700°C) as a result of the crystallization of the amorphous phase. Nearly constant $M_{H=18koe}$ were observed for temperatures higher than 700°C, suggesting although phase transformation exist at higher temperatures, the change in the relative phase content might not be large enough to create observable changes in the overall magnetization at 18kOe.

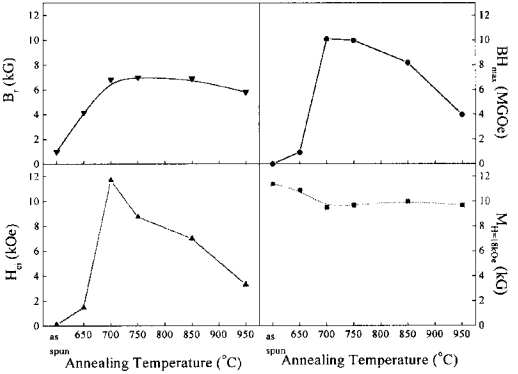

Figure 1. Magnetic properties of as-melt-spun and thermally processed $(Nd_{0.95}La_{0.05})_{9.5}Fe_{bal}Co_5Nb_2B_{10.5}$.

Shown in Figure 2 are the TMA scans of the samples studied. The as-spun and the 650°C treated materials show a large amount of the unknown phase with a T_c of 170°C. The low H_{ci} values obtained on these two samples suggest that this amorphous phase is indeed a soft magnetic phase. During crystallization, this soft and amorphous phase transformed into phases dictated by the nominal alloy composition and the phase transformation paths. Two magnetic phases, namely, $Nd_2(Fe\ Co)_{14}B$ and α-(Fe Co) (for α-Fe, T_c~770°C) were detected on samples treated at 700°C. When treated at 750°C, the amount of α-Fe increased slightly and a traceable amount of Fe_3B (T_c~510°C) was also detected. This increase in the amount of α-Fe is consistent with the slight increase in B_r observed. At 850°C, the amount of Fe_3B decreased significantly suggesting that Fe_3B may transform into some other, possibly non-magnetic, phases. Additional test at 950°C exhibited consistent trend of decrease of Fe_3B with the thermal treatment temperatures. It should be noted that the T_c of $Nd_2(Fe\ Co)_{14}B$ increased as a function of the thermal processing temperatures. When processed at 650, 700, 750, 850°C, and 950°C, the T_c of $Nd_2(Fe\ Co)_{14}B$ was 343°C, 351°C, 367°C, 395°C, and 410°C, respectively. The cause of this change in T_c is not clear at this point. Phase transformation from $Nd_2(Fe\ Co)_{14}B$ is unlikely based on the XRD data shown in Figure 3. However, the decrease in the amount of the α-Fe and Fe_3B may result in a redistribution of the Co in the nanocomposites. The increase of the Co content in the $Nd_2(Fe\ Co)_{14}B$ may therefore in turn explain the increase of its Curie temperature with the thermal treatment temperatures.

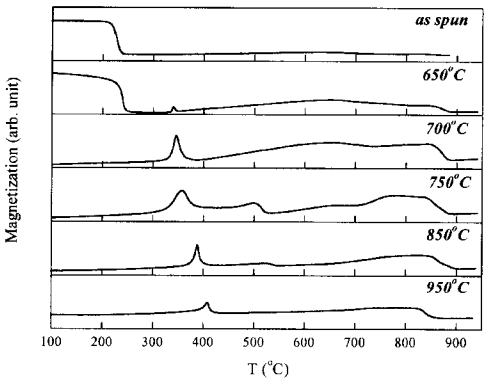

Figure 2. TMA scans of the as-melt-spun and thermally processed $(Nd_{0.95}La_{0.05})_{9.5}Fe_{bal}Co_5Nb_2B_{10.5}$.

Shown in Figure 3(a) are the XRD scans of the samples treated with various thermal processing temperatures. Evolution of the crystallization from amorphous material to a composite of $Nd_2(Fe\ Co)_{14}B$ and α-Fe were demonstrated. To compare the growth rate of $Nd_2(Fe\ Co)_{14}B$ and α-Fe, the intensities of the (410) peak of the $Nd_2(Fe\ Co)_{14}B$ phase and the (110) peak of the α-Fe phase

were plotted against the temperature in Figure 3(b). It can be seen that most of the crystallization of the $Nd_2(Fe\ Co)_{14}B$ phase occurred at temperature lower than 700°C, while the growth of the α-Fe phase accelerated as the temperature rose.

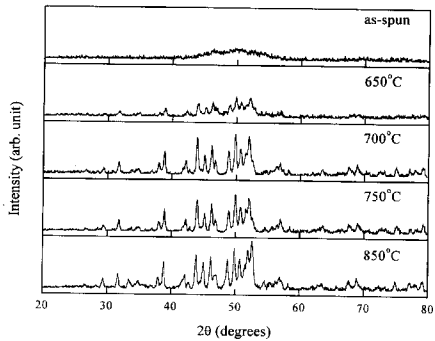

(a)

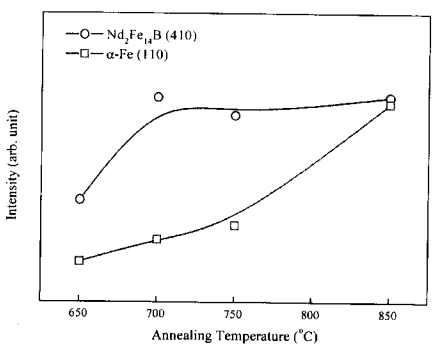

(b)

Figure 3. (a) XRD of as-spun $(Nd_{0.95}La_{0.05})_{9.5}Fe_{bal}Co_5Nb_2B_{10.5}$. (b) Intensities of the (410) peak of $Nd_2(Fe\ Co)_{14}B$ and the (110) peak of α-Fe versus the temperature.

Shown in Figure 4 are the ΔM-versus-H of samples included in this study. To illustrate the effect of grain size on this type of plot, a ΔM versus H curve of a sintered NdFeB with an average grain size of 10 μm, pulverized to an equivalent powder size, was also included for comparison. As expected, the crushed sintered NdFeB showed mostly negative ΔM, suggesting a magnetostatic-dominated particle interaction[7,8]. The ΔM of the as-melt-spun materials and samples heat treated at 650°C exhibited similar behavior. For samples treated above 650°C, a positive ΔM was observed indicating the existence of exchange coupling between phases[7,8,10]. The height of the ΔM peak reached a maximum when materials were treated at 700°C, suggesting the strongest exchange coupling among samples studied. At 750 and 850°C, the peaks of ΔM decreased significantly, an indication of a weakened exchange interaction. Microstructural examinations, both on average grain size and phase distribution, are necessary to quantify this change in exchange coupling. We should also point out that unlike the classical exchange coupling case where the system is composed of 60% hard magnetic phases and 40% of soft magnetic phases [4], the system involved in this study is composed of more than 90% of the hard magnetic phase, determined by the nominal composition used in this study. The purpose is to maintain relatively higher H_{ci}, while still being able to have an exchange-coupled nanocomposite system to study.

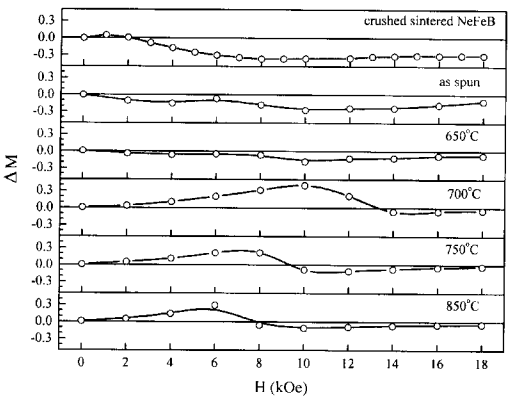

Figure 4. The ΔM-versus-H plots of the sintered $Nd_{15}Fe_{79}B_6$ and as-melt-spun and thermally processed $(Nd_{0.95}La_{0.05})_{9.5}Fe_{bal}Co_5Nb_2B_{10.5}$.

Table I. The average grain sizes obtained from TEM images.

sample	average grain size (nm)	
	primary phase	secondary phase
as-spun	n/a	n/a
650°C	38	n/a
700°C	40	n/a
750°C	45	5
850°C	68	12

Shown in Figure 5 are the TEM images and the inset EDP of samples in the as-spun state and after thermal treatments at 650°C, 700°C and 750°C. The as-spun sample, shown in Figure 5(a), appeared to be homogenous and showed no crystal grain. The amorphous material observed agreed well with our results from TMA and XRD reported earlier in this paper. After thermal treatment at 650°C, we observed $Nd_2(Fe\ Co)_{14}B$ grains embedded in a large amount of amorphous residual, indicating a partial crystallization occurred at 650°C (see Figure 5(b)). At 700°C, shown Figure 5(c), more well-defined grains could be observed and the elimination of the amorphous phase was noticed. The development of soft phases and some secondary phases became more prevalent in samples treated at temperatures higher than 700°C. TEM images at 750°C are shown in Figure 6(a) and (b). Some observable small precipitates started to develop at the grain boundaries as intergranular phases (black arrows in Figure 6(b)). At 850°C, as these intergranular phases grew, they were able to be identified as either α-Fe or Fe_3B, using micro-diffraction technique. See Figure 7(a) and (b). Interestingly, new phase(s) started to precipitate within the $Nd_2(Fe\ Co)_{14}B$ grains at 850°C. Due to the small grain size of these grains, they have not been characterized by either electron diffraction or elemental analysis at this point. Since no additional ferromagnetic phase was observed in the TMA scan for 850°C, we suspected that the new precipitate may actually be non-magnetic phases, such as borides.

The development of the primary and secondary phases as well as the grain growth can be reflected by the change in the grain size distributions. Descriptive statistical data on the grain sizes were obtained from the TEM images. Shown in Figure 8 are the grain size distribution of samples thermally treated from 650°C to 850°C. At 650°C, a symmetrical single peak distribution was observed. The distribution became biased to the smaller grain size at 700°C, which could be an indicator of the formation of the bi-modal distribution found in samples at 750°C. Listed in Table I are the average grain sizes of the primary and secondary phases determined [1]. It suggests that the as-spun materials are fully amorphous. Grain growth from 650°C (38nm) to 700°C (40nm), was not significant. At 750°C, the grain size of the primary phase increased to 45nm and newly developed intergranular phases resulted in a second peak averaged at 5nm. At 850°C, the primary phase and the secondary phase peaks shifted to the larger grain size, i.e., 68nm, and 12nm, respectively. It is of interest that the grain size of the primary phase, $Nd_2(Fe\ Co)_{14}B$ grains, did not increase significantly until 850°C. It is then suspected that the intergranular precipitates may serve as barriers at the grain boundaries to prevent the $Nd_2(Fe\ Co)_{14}B$ grain coarsening [1].

Our microstructure analyses agree well with the magnetic performances as well as the strength of the exchange coupling interaction between the $Nd_2(Fe\ Co)_{14}B$ and α-Fe, Fe_3B phases characterized by the ΔM-versus-H plot. The optimal magnetic performance occurred between 700°C and 750°C, where no amorphous phase is left, no excessive grain growth has started, and

reasonable fraction of soft phase is present. The highest ΔM was found a 700°C where the crystallization was just completed and smallest average grain size was observed. The highest ΔM, representing the strongest exchange interaction, occurred at the same temperature as did H_{ci}. However, the optimal magnetic performance, namely, BH_{max}, appeared to stay at the same level between 700°C and 750°C, where B_r increased at the expense of H_{ci}. This resulted from the fact that the optimal magnetic properties are not only impacted by the strength of the exchange interaction, but also dictated by the relative content of various phases of the composite.

The 2% Nb addition in our composition is also of our interest. While we found that Nb is very effective in improving the H_{ci} of the system, the actual location of Nb in terms of microstructure is not clear at this point. We suspect Nb may be present in forms of various borides and serve as pinning centers for the domain walls during the demagnetizing process. However, we were unable to identify them via XRD due to their extremely small volume fractions, if any was present. The precipitation developed within the grains of primary phase was also suspected to be related to the Nb addition. Works on identifying them are currently underway and we will report our progress in the near future.

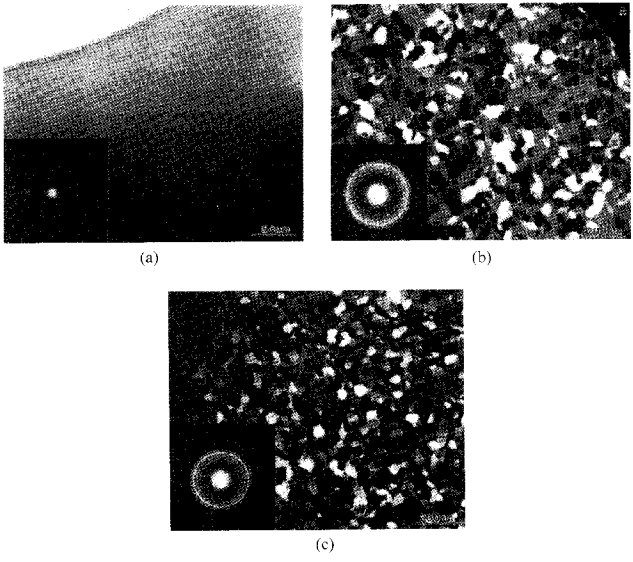

(a) (b)

(c)

Figure 5. TEM images of ribbons in as-spun state and after thermal treatments. (a) As-spun. (b) 650°C. (c) 700°C.

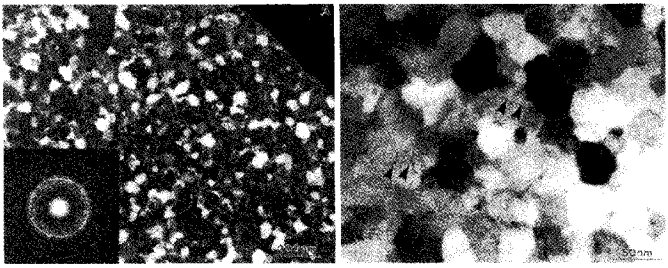

(a) (b)

Figure 6. TEM images of ribbons after thermal treatments at 750°C. (a) Lower magnification. (b) Higher magnification. Black arrows point to intergranular phases.

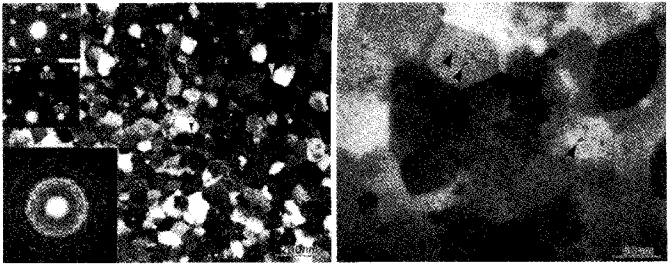

(a) (b)

Figure 7. TEM images of ribbons after thermal treatments at 850°C. (a) Lower magnification. (b) Higher magnification. Black arrows point to new phase(s) precipitated within $Nd_2(Fe\ Co)_{14}B$ grains.

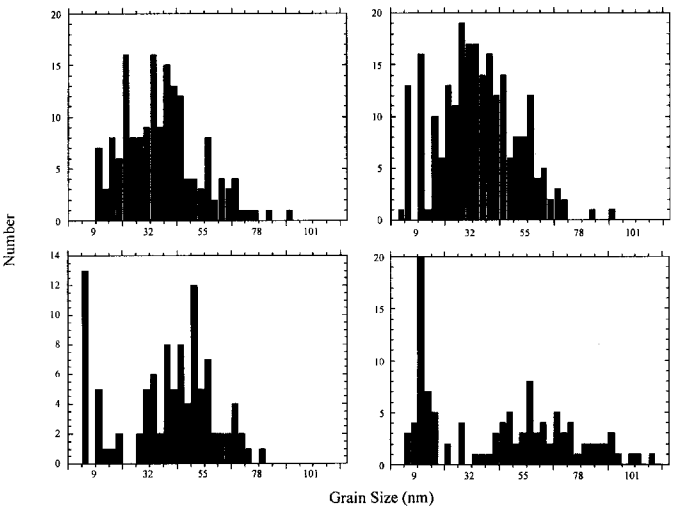

Figure 8. Grain size analyses from TEM images for thermally treated ribbons. Top left: 650°C. Top right: 700°C. Bottom left: 750°C. Bottom right: 850°C.

CONCLUSIONS

The effects of phase transformations and microstructures on the magnetic properties of $(Nd_{0.95}La_{0.05})_{9.5}Fe_{bal}Co_5Nb_2B_{10.5}$ nanocomposites has been investigated systematically. It was found that B_r, H_{ci}, and BH_{max} obtained were affected by the magnetic phases present as well as the strength of the exchange coupling. The optimal magnetic performance, BH_{max}, occurred between 700C to 750°C, where the crystallization has completed without excessive grain growth. TMA and TEM indicated that the system was composed of three phases at this point, $Nd_2(Fe\ Co)_{14}B$, α-Fe, and Fe_3B. The ΔM-versus-H plot successfully interpreted the effect of the exchange coupling on B_r, H_{ci}, and BH_{max} obtained for samples treated below 750°C. While similar ΔM-H curves were obtained for samples treated at higher than 750°C, degradation in B_r, H_{ci}, and BH_{max} was found. This degradation may be attributed to the grain growth of the main phases, from 45 to 68nm, and the development of precipitates developed within the $Nd_2(Fe\ Co)_{14}B$ grains. It was hypothesized that the precipitated phases could be finely dispersed borides. The formation of these borides, in conjunction with the mass balance, may explain the increase in the T_c of $Nd_2(Fe\ Co)_{14}B$ and the decreased amount of α-Fe and Fe_3B when thermally processed at temperatures above 700°C.

REFERENCES

[1] B. Lu, M.Q. Huang, Q. Chen, B.M. Ma, and D.E. Laughlin, Proc. Of 43rd Annual Conference on Magnetism and Magnetic Materials, Miami, Florida (1998), in press.

[2] E. F. Kneller and R. Hawig, IEEE Trans. Mag. **27**, p.3588 (1991).

[3] R. Skomski and J. M. D. Coey, *Phys. Rev. B* **48**, p.1581 (1993).

[4] T. Schrefl, J. Fidler, and H. Kronmuller, *Phys. Rev. B*, **49**, p.6100 (1994).

[5] R. Fischer, T. Schrefl, H. Kronmuller, and J. Fidler, *J. Magn. Magn. Mater.* **153**, p.35 (1996).

[6] J. Ormerod, S. Constantinides, J. Appl. Phys. **81**, p.4816 (1997).

[7] E. P. Wohlfarth, J. Appl. Phys. **29**, p.595 (1958).

[8] P. E. Kelly, K. O. Grady, P. I. Mayo, and R. W. Chantrell, IEEE Trans. Mag. **25**, p.3881 (1989).

[9] M. Fearon, R. W. Chantrell, E.P.Wohlfarth, *J. Magn. Magn. Mater.* **86**, p.197 (1990).

[10] W. C. Chang, S. H. Wu, B. M. Ma, C. O. Bounds, S. Y. Yao, J. Appl. Phys. **83**, p.2147 (1998).

[11] Manaf, R. A. Buckley, and H. A. Davies, J. Magn. Magn. Mater. **128**, p.302 (1993).

[12] L. Withanawasam, A.S. Murphy, G. C. Hadjipanayis, K. R. Lawles, R. F. Krause, J. Magn. Magn. Mater. **140-145**, p.1057 (1995).